

Electric-Field-Induced Molecular Alignment of Side-Chain Liquid-Crystalline Polyacetylenes Containing Biphenyl Mesogens

JIANXIN GENG,¹ ENLE ZHOU,¹ GAO LI,¹ JACKY WING YIP LAM,² BEN ZHONG TANG²

¹State Key Laboratory of Polymer Physics and Chemistry, Changchun Institute of Applied Chemistry, Chinese Academy of Sciences, Changchun 130022, China

²Department of Chemistry, Hong Kong University of Science & Technology, Clear Water Bay, Kowloon, Hong Kong, China

Received 8 September 2003; revised 6 November 2003; accepted 1 December 2003

ABSTRACT: Electric-field-induced molecular alignments of side-chain liquid-crystalline polyacetylenes $[-(\text{HC}=\text{C}[(\text{CH}_2)_m\text{OCO-biph-OC}_7\text{H}_{15}])_n-]$, where biph is 4,4'-biphenyl and m is 3 (PA3EO7) or 9 (PA9EO7)] were studied with X-ray diffraction and polarized optical microscopy. An orientation as high as 0.84 was obtained for PA9EO7. Furthermore, the molecular orientation of PA9EO7 was achieved within a temperature range between the isotropic-to-smectic A transition temperature and 115 °C, and this suggested that the orientational packing was affected by the thermal fluctuation of the isotropic liquid and the mobility of the mesogenic moieties. The maximum achievable orientation for PA9EO7 was much greater than that for PA3EO7. This was the first time that the electric-field-induced molecular orientation of a side-chain liquid-crystalline polymer with a stiff backbone was studied. © 2004 Wiley Periodicals, Inc. *J Polym Sci Part B: Polym Phys* 42: 1333–1341, 2004

Keywords: side-chain liquid-crystalline polymers; polyacetylenes; orientation; electric field; X-ray

INTRODUCTION

It is well known that the molecular alignment of liquid-crystalline polymers can be achieved within the temperature range of the liquid-crystalline phase with a magnetic field, an electric field, surface shearing, and a stretching effect and then be preserved by the simple cooling of the polymer to its glassy or crystalline state.^{1–5} In the literature, the reports on external-field-induced molecular orientation are mainly focused on main-chain liquid-crystalline polymers and side-chain liquid-crystalline polymers with soft back-

bones.^{6–8} Side-chain liquid-crystalline polymers with stiff backbones (e.g., side-chain liquid-crystalline polyacetylenes, polypyrroles, and polythiophenes) have attracted much interest from scientists in recent years.^{9–17} Because of the long relaxation time of the rigid polyacetylene backbone, the twisted conformation cannot quickly relax back to the original state after shearing, and this enables the easy observation of schlieren textures with high-strength disclinations, inversion walls, and banded textures.^{18,19} The alignment of the polymer conjugated main chains accompanying mesogen orientation induced by a magnetic field can improve the conductivity in the direction of the aligned backbone and give rise to remarkable electrical anisotropy.^{20–23}

Correspondence to: G. Li (E-mail: ydh@ns.ciac.jl.cn)

Journal of Polymer Science: Part B: Polymer Physics, Vol. 42, 1333–1341 (2004)
© 2004 Wiley Periodicals, Inc.

As part of our efforts to understand the external-field-induced molecular orientation of side-chain liquid-crystalline polyacetylenes, we have recently proposed an orientation mechanism of a side-chain liquid-crystalline polyacetylene, poly(11-[[4'-heptoxy-4-biphenyl]carbonyl]oxy)-1-undecyne) (PA9EO7), induced by a shear force.¹⁹ At its smectic A (S_A) phase, as an orienting unit, the polymer main chain can align parallel to the direction of the shear flow. However, because of the bad fluidity, only layer planes of the smectic phase can glide parallel to the shear direction at its high order smectic phase; this leads to an orientation of the biphenyl mesogens parallel to the shear direction.

To further investigate the external-field-induced orientation mechanism of side-chain liquid-crystalline polyacetylenes, here we report a systematic study of the electric-field-induced molecular orientation behavior of PA9EO7 and poly(5-[[4'-heptoxy-4-biphenyl]carbonyl]oxy)-1-pentyne) (PA3EO7) with polarized optical microscopy (POM) and X-ray diffraction (XRD).

EXPERIMENTAL

Instrumentation

Optical microscopy observation experiments were carried out with a Leica POM instrument equipped with a TMS 94 hot stage produced by Linkam Scientific Instruments, Ltd., in the cross-polarized mode. XRD patterns were recorded on a Rigaku D/max 2500 PC diffractometer with an R-Axis DS3 X-ray data collection system with X-rays from Cu $K\alpha$ radiation with a wavelength of 1.54056 Å. The R-Axis DS3 is an X-ray data collection system with an imaging plate (IP). It reads an XRD pattern imaged over the IP surface and loads it into the host computer as digital data. The IP is a storage radiation detector. It stores incident radiation energy and allows one to read the stored energy. The camera length used in the XRD pattern imaging is 118 mm. The transmission electron microscopy (TEM) observations and electron diffraction (ED) patterns of PA3EO7 sample were made on a JEOL 2010 TEM instrument operating at 200 kV.

Specimen Preparation

The chemical structure of the mesogenic polyacetylenes used in this study is shown in Figure 1. The synthesis and mesomorphic properties were

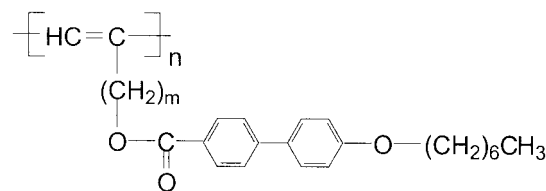


Figure 1. Molecular structure of PA3EO7 ($m = 3$) and PA9EO7 ($m = 9$).

reported in our previous articles.^{24,25} The phase sequences for these two polymers were as follows: for PA9EO7, smectic B (S_B) 75.6 °C S_A 128.6 °C isotropic (on heating) and isotropic 127.6 °C S_A 74.1 °C S_B (on cooling), and for PA3EO7, glassy 102.2 °C smectic 180.7 °C isotropic (on heating) and isotropic 174.4 °C smectic 100.1 °C glassy (on cooling). The distances between the layer planes of the S_A and S_B phases of PA9EO7 were 32.57 and 33.82 Å, respectively, and the lateral distances of the biphenyl mesogens of the two smectic phases were both 4.4 Å. As for molecular packing at the smecticity, the mesogens on the one side of one polymer overlapped on the mesogens on the other side of the neighboring polymer in an antiparallel overlapping manner.^{25,26} Under POM observation, S_A phase-separated out in the form of a bâtonnet texture when PA9EO7 cooled from its isotropic melt. Accompanying a further reduction in the temperature, bâtonnets coalesced and built up the focal-conic texture. A broken focal-conic texture evolved when PA9EO7 reached the S_B phase. The alignment of the bâtonnets, focal-conic texture, and broken focal-conic texture were completely irregular.

PA3EO7 was dissolved in toluene to make 0.05 wt % solutions. The solutions were dropped onto thin carbon films precoated on a surface of freshly cleaved mica. After the solvent evaporated, the thin solid films were obtained. The PA3EO7 films were heated up to melting, cooled, and then quenched by liquid nitrogen to freeze the molecular arrangements in the liquid-crystalline phase. The samples were transferred onto copper grids, which were analyzed with ED and morphology observation with a TEM instrument.

Molecular alignment induced by an electric field was performed with a homemade device shown in Figure 2. Aluminum electrodes were deposited on a glass slide *in vacuo*. The specimens were placed between the two Al electrodes and then heated up to melting. The specimens were kept well above the clear point for 15 min to

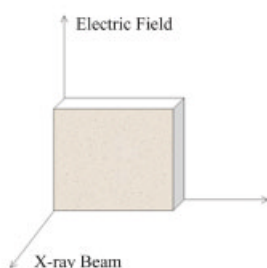
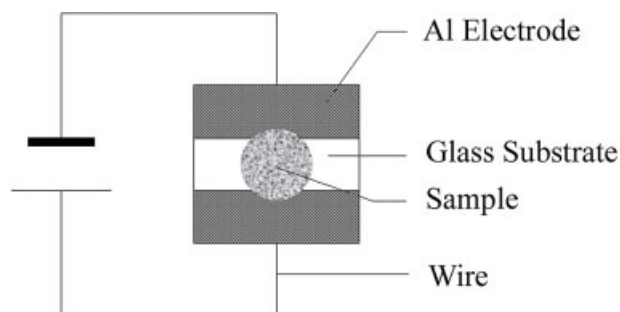


Figure 2. Homemade electrode and a scheme showing the X-ray incident normal to the direction of the electric field.

ensure perfect isotropic liquids. A direct electric field was applied to the device when the specimens were cooled from their isotropic state or mesophase. Electric-field-induced molecular packing orientation was preserved when the specimens were cooled to room temperature, and the orientation degree was measured with XRD experiments with the X-ray beam incident normal to the direction of the applied electric field (Fig. 2). As for POM experiments, *in situ* observations were made when the specimens cooled from their isotropic melt and the applied electric field was maintained.

RESULTS AND DISCUSSION

Electric-Field-Induced Molecular Orientation

To obtain direct information on the electric-field-induced molecular packing arrangement, we observed the orientation behavior of the mesomorphic texture with POM. When PA9EO7 was

cooled from its isotropic melt, a bâtonnet texture with an average diameter of $4.5\ \mu\text{m}$ was observed around $127\ ^\circ\text{C}$, as shown in Figure 3(a). The bâtonnets were randomly oriented. The orientation of the polarizer and analyzer is shown by the bidirectional arrow in the image. All the following POM images were obtained in this orientation of the polarizer and analyzer. Figure 3(b–f) shows the increase of the order degree of the texture with an increase in the electric-field strength. The dark regions in these images represent the aluminum electrodes. The bottom left part is the cathode, and the top right part is the anode. When the intensity of the electric field reached $2.5 \times 10^5\ \text{V m}^{-1}$, the mesomorphic texture exhibited a perfect alignment parallel to the direction of the elec-

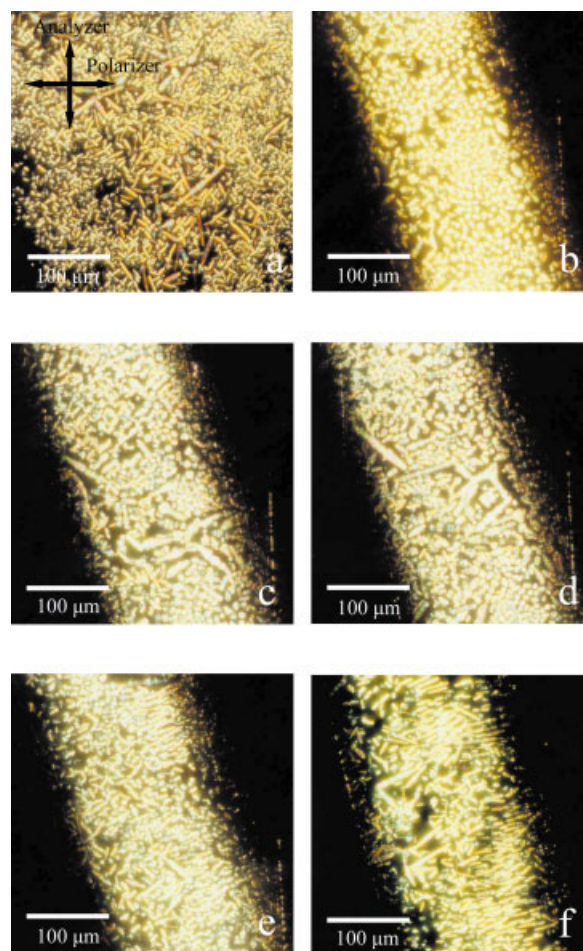


Figure 3. Orientation of bâtonnets of PA9EO7 as a function of the electric field when the S_A phase separates from the isotropic melt. The strengths of the applied electric fields are (a) 0, (b) 6.25×10^4 , (c) 1.25×10^5 , (d) 1.875×10^5 , (e) 2.5×10^5 , and (f) $3.125 \times 10^5\ \text{V m}^{-1}$.

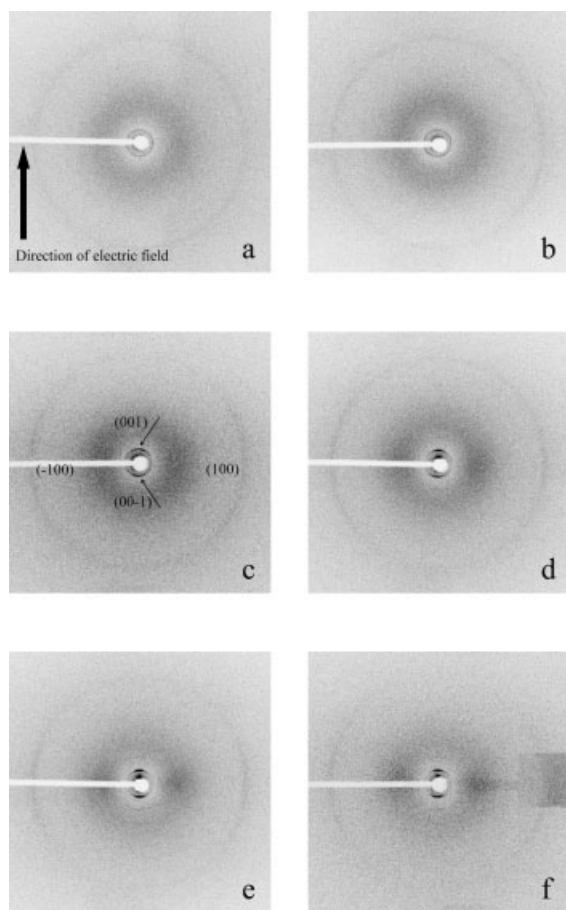


Figure 4. XRD patterns of oriented PA9EO7 obtained at electric-field intensities of (a) 0, (b) 6.25×10^4 , (c) 1.25×10^5 , (d) 1.875×10^5 , (e) 2.5×10^5 , and (f) $3.125 \times 10^5 \text{ V m}^{-1}$.

tric field. When PA9EO7 was cooled from its isotropic liquid, a liquid-crystalline nucleus appeared, with the long axis parallel to the direction of the applied electric field. The newborn nuclei grew from their tips to form bâtonnets, or smaller nuclei added onto the tips of bigger ones.

With the aid of X-ray experiments, we obtained orientation information on the molecular level. The specimens were prepared as follows. PA9EO7 samples were heated in the homemade device up to isotropic melting (160°C), and an electric field with a designated intensity was applied to the device. After 15 min, the specimens were cooled to room temperature, with the applied electric field maintained. Figure 4 shows the XRD patterns of PA9EO7 at the electric-field strengths of 0, 6.25×10^4 , 1.25×10^5 , 1.875×10^5 , 2.5×10^5 , and $3.125 \times 10^5 \text{ V m}^{-1}$. Derived from the Bragg law, the XRD rings or arcs closer to the incident X-ray

beam corresponded to the distance between the layer planes of the S_B phase ($d = 33.82 \text{ \AA}$), whereas the diffuse XRD rings far from the incident X-ray beam corresponded to the lateral intermolecular distance of the mesogens ($d = 4.4 \text{ \AA}$). The XRD ring at a low angle separated into two arcs parallel to the direction of the applied electric field when the electric field reached $1.875 \times 10^5 \text{ V m}^{-1}$ [Fig. 4(c)]. The diffraction ring corresponding to the lateral distance of the biphenyl mesogens also divided into two arcs normal to the direction of the applied electric field. The order degree increased with an increase in the intensity of the applied electric field. This result suggested that the electric field induced the biphenyl mesogenic moieties parallel to the direction of the applied electric field in the process of the growth of the mesomorphic texture. In our previous studies,^{25,26} the direction of the molecular long axis of biphenyl was normal to the polyacetylene main chain. Thus, the polyacetylene backbones were normal to the direction of the applied electric field. Figure 5 presents a model of the molecular arrangement under an electric field. The direction of the molecular long axis of the biphenyl mesogens is parallel to the direction of the electric field. Referring to the experimental results shown in Figure 3, we find that the orientation of the biphenyl mesogenic moieties is in agreement with that of the bâtonnet texture, and this indicates that the mesomorphic texture grows with the direction of the long molecular axis of the biphenyl mesogens parallel to the direction of the bâtonnets.

Of particular interest is the influence of the temperature on the molecular orientation. Keeping the specimens at 160°C for 15 min ensured the initial isotropic state for each measurement. The specimens were cooled to a designated temperature, and then an electric field with an intensity of $3.5 \times 10^5 \text{ V m}^{-1}$ was applied. After 15 min, the specimens were cooled to room temperature to preserve the molecular orientation, and the applied electric field was maintained. The electric field clearly contributed to the molecular packing orientation from the moment when it was applied, that is, from the designated temperature to room temperature. Figure 6 shows a series of XRD patterns of an oriented PA9EO7 specimen when the electric field was applied at 135, 130, 125, 120, 115, and 110°C . The molecular packing orientation obviously decreased as the applied temperature was lowered. The order degree was almost lost when the electric field was applied at 110°C .

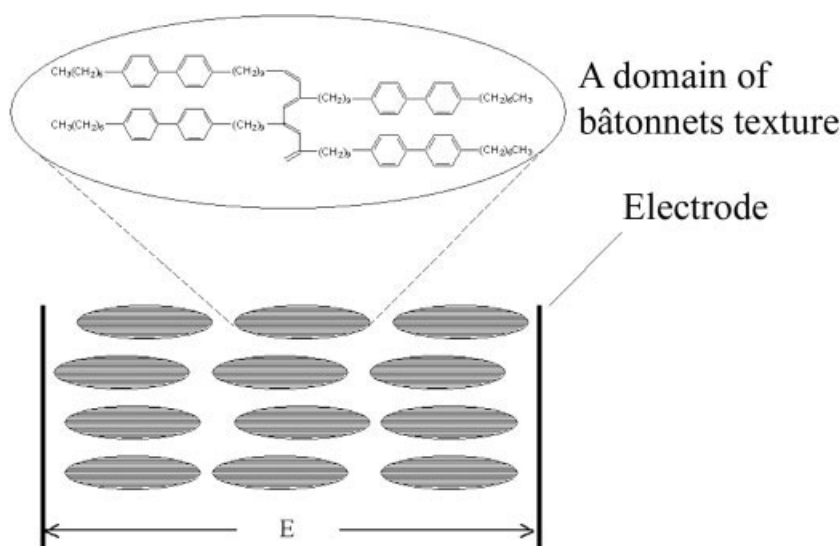


Figure 5. Molecular packing model of electric-field-induced PA9EO7.

[Fig. 6(f)] because of the lack of mobility of the biphenyl mesogenic moieties.

In another set of experiments investigating the influence of the temperature on the molecular orientation, a specimen was cooled to a designated temperature, and an electric field with an intensity of $3.5 \times 10^5 \text{ V m}^{-1}$ was then applied. After 1 h, the specimen was quenched with liquid nitrogen to freeze the aligned molecular arrangement. The dependence of the electric-field-induced molecular packing on the orientation temperature is shown in Figure 7. The molecular alignment of PA9EO7 took place just below the isotropic-to- S_A transition temperature, 127.5°C [Fig. 7(b)], and the orientation degree was strongly affected by the oriented temperature. The oriented molecular arrangement disappeared when the orientation temperature reached 115°C [Fig. 7(g)]. This result seems to reflect the influence of the mobility of the biphenyl mesogenic moieties and the thermal fluctuations of the isotropic melt.

Spacers play an important role in decoupling the interaction between the polymer main chain and mesogens.^{27,28} To evaluate the influence of the spacer on the molecular orientation of biphenyl mesogens, we investigated PA3EO7 possessing a shorter spacer than PA9EO7. PA3EO7 yielded a complicated molecular packing arrangement. Figure 8 shows a liquid-crystalline domain and its *in situ* ED pattern with the electron beam incident parallel to the layer planes of the smecticity. The two-dimensional ED pattern may de-

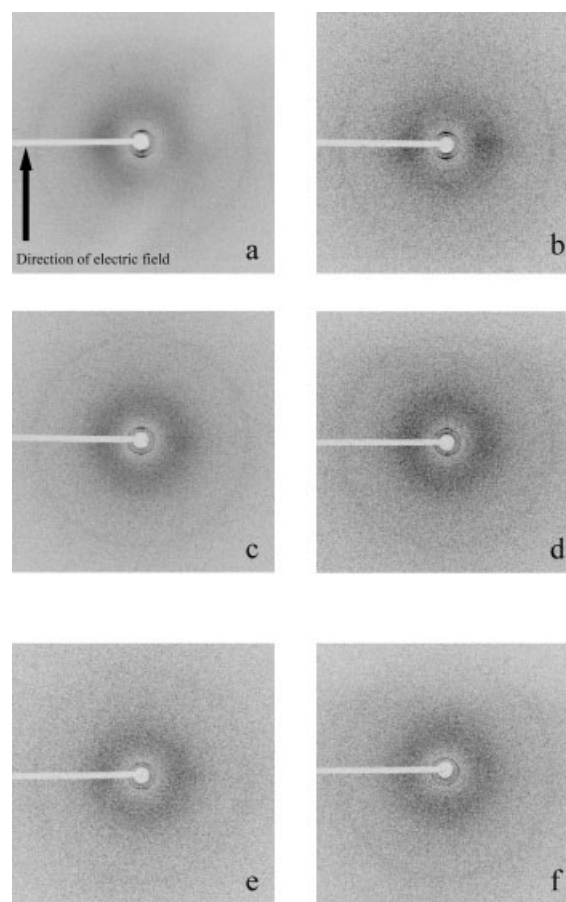


Figure 6. Orientation degree of PA9EO7 decreasing with decreasing temperature when an electric field is applied: (a) 135°C , (b) 130°C , (c) 125°C , (d) 120°C , (e) 115°C , and (f) 110°C .

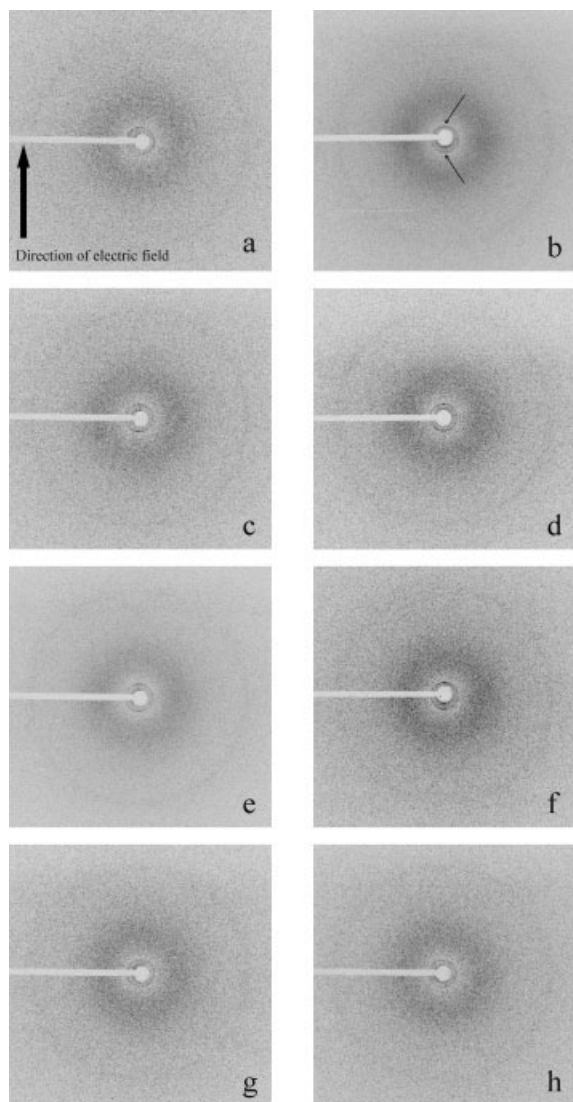


Figure 7. Orientation of XRD patterns of PA9EO7 as a function of the orientation temperature: (a) 130, (b) 127.5, (c) 125, (d) 122.5, (e) 120, (f) 117.5, (g) 115, and (h) 110 °C.

rive from a kind of supermolecular structure, and d -spacings of 29.82 and 23.66 Å were calculated from ED spots 1 and 2, respectively. Here we only report the experimental phenomenon; how the molecules pack in this phase is currently under investigation.

Figure 9 shows XRD patterns of an electric-field-induced PA3EO7 specimen at intensities of 6.25×10^4 , 1.25×10^5 , 1.875×10^5 , 2.5×10^5 , 3.125×10^5 , 3.75×10^5 , 4.375×10^5 , and 5×10^5 V m⁻¹. The XRD ring closer to the incident beam corresponded to ED spot 1, and the XRD ring or arcs far from the incident beam corresponded to

ED spot 2 [Fig. 8(b)]. The outer ring with a d -spacing of 23.66 Å had a slight orientation when the electric field reached 2.5×10^5 V m⁻¹. The molecular orientation of the mesogenic moieties developed with an increase in the intensity of the applied electric field. The order degree reached a maximum value when the electric field was increased to 4.375×10^5 V m⁻¹ [Fig. 9(g)]. However, the development of the molecular orientation with an increase in the electric field was obviously slower than that of PA9EO7. The intensity of the applied electric field giving the maximum molecular orientation was greater than that for PA9EO7. However, the inner ring corresponding to the d -spacing of 29.82 Å had no obvious orientation throughout the process.

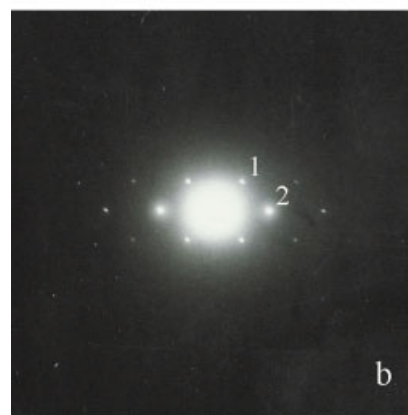
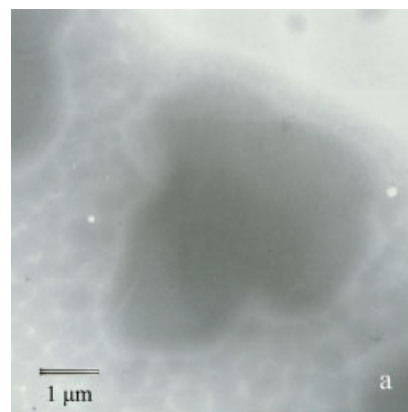


Figure 8. Morphology and *in situ* ED pattern of PA3EO7 with the electron beam incident normal to the layer planes of smecticity.

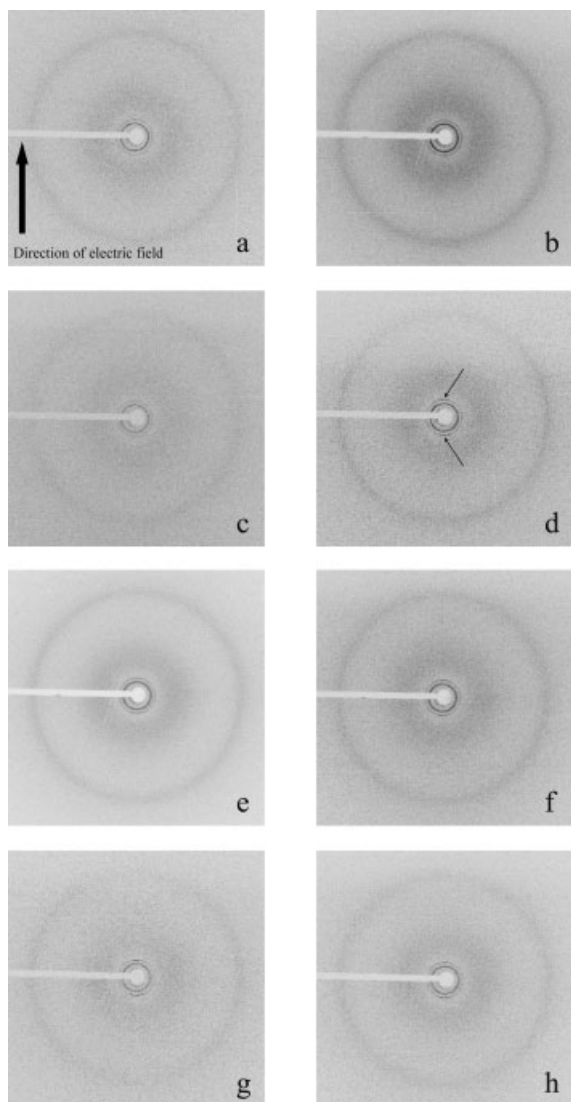


Figure 9. Orientation of XRD patterns of PA3EO7 as a function of the applied electric field. The strengths of the applied electric field are (a) 6.25×10^4 , (b) 1.25×10^5 , (c) 1.875×10^5 , (d) 2.5×10^5 , (e) 3.125×10^5 , (f) 3.75×10^5 , (g) 4.375×10^5 , and (h) $5 \times 10^5 \text{ V m}^{-1}$.

Calculation of the Order Parameter

IP imaging technology can convert a two-dimensional XRD pattern into a one-dimensional X-ray diffractogram with an azimuth. We define the incident X-ray beam as the center and draw two homocentric circles, the diffraction angles (2θ) of which differ by 1° , to make a torus that covers the diffraction ring or arcs, as shown in Figure 10(a). Digital information of the diffraction intensity on the torus can be read clockwise from the arrow-marked line with a step of 1° . Then, the collected diffraction intensity is plotted as a function of the

azimuth in Figure 10(b). The two halves of the diffraction peaks at 0 and 360° correspond to the diffraction arc above the incident X-ray beam [Fig. 10(a)], and the diffraction peak at 180° corresponds to the diffraction arc below the incident X-ray beam. The diffraction peak at 180° is fitted with a Gaussian formula to obtain a smoothed peak. It allows us to determine the order parameter π , which is defined as $\pi = [(180 - H)/180] \times 100\%$, in which H is the width at the half-height of the Gauss fitted peak. The order parameter π is a measure of the average orientation over all molecular units being studied and ranges from 0 , for

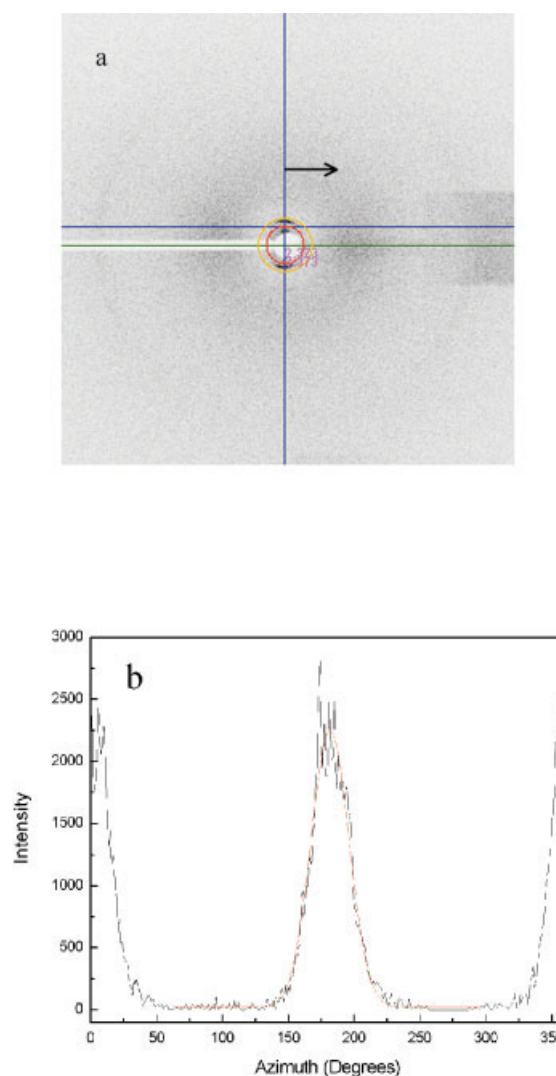


Figure 10. Transformation from a two-dimensional XRD pattern into a one-dimensional azimuth curve: (a) the two-dimensional XRD pattern and (b) the diffraction intensity (collected along the torus) drawn as a function of the azimuth.

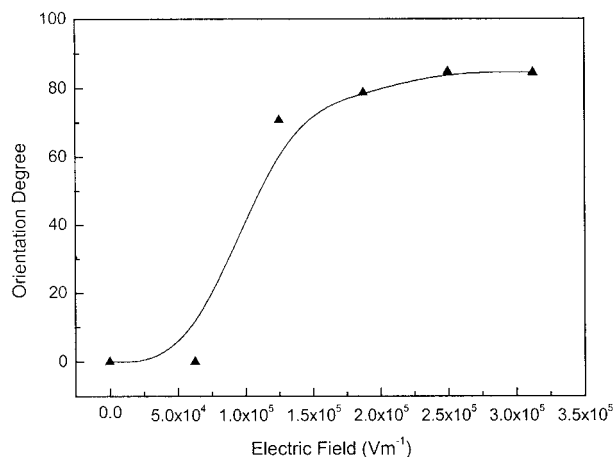


Figure 11. Order parameter of oriented PA9EO7 as a function of the applied electric field.

a random orientation, to 1, for a perfect orientation. H is 180 for a random orientation and 0 for a perfect orientation.

Figure 11 shows the change of the order parameter calculated from Figure 4 as a function of the intensity of the electric field. It is a typical S-shaped curve. At the beginning of the curve, the biphenyl mesogenic moieties are randomly oriented. The orientation degree of the mesogens increases rapidly when the electric field intensity goes to $1 \times 10^5 \text{ V m}^{-1}$. With a further increase in the electric field, the order parameter reaches a maximum value of $\pi_{\text{max}} = 0.84$. The precision of the order parameter calculated with this method is intensively dependent on the intensity of the diffraction arc. Deviation exists in the determination of H when the diffraction arc is relatively weak, thus leading to a deviation in the calculation of π . In the case of a misleading reader, we do not do the same analysis for Figures 6, 7, and 9.

CONCLUSIONS

Using a POM instrument equipped with a home-made electrode, we observed the electric-field-induced bâtonnet alignment of polyacetylene with biphenyl mesogenic moieties. The long axis of the bâtonnet texture was parallel to the direction of the applied electric field. X-ray diffractograms provided information on the molecular packing arrangement. Our analysis indicated that the long molecular axis of the biphenyl mesogenic moieties packed parallel to the direction of the applied electric field and that the polymer back-

bone was normal to the direction of the applied electric field. Furthermore, antagonistic action between the randomization caused by the thermal fluctuation in the isotropic melt and the orientation induced by the electric field in the liquid-crystalline phase was a key factor to tune to obtain the favorite molecular orientation. The maximum achievable orientation of PA9EO7 was much greater than that of PA3EO7, whereas the strength of the electric field required for generating the maximum order degree for PA9EO7 was much smaller than that for PA3EO7.

The authors thank the National Natural Science Foundation of China (29904008, 20174043, and 20023003) and the Research Grants Council of Hong Kong (HKUST6121/01P and 6085/02P) for their financial support. This work was also subsidized by the Special Funds for Major State Basic Research Projects.

REFERENCES AND NOTES

1. Roche, P.; Zhao, Y. *Macromolecules* 1995, 28, 2819–2824.
2. Zhao, Y.; Roche, P.; Yuan, G. *Macromolecules* 1996, 29, 4619–4625.
3. Xu, Z. S.; Lemieux, R. P.; Natansohn, A.; Rochon, P.; Shashidhar, R. *Chem Mater* 1998, 10, 3269–3271.
4. Romo-Uribe, A.; Windle, A. H. *Macromolecules* 1996, 29, 6246–6255.
5. Dadmun, M. D.; Clingman, S.; Ober, C. K.; Nakatani, A. I. *J Polym Sci Part B: Polym Phys* 1998, 36, 3017–3023.
6. Sanger, J.; Gronski, W.; Leist, H.; Wiesner, U. *Macromolecules* 1997, 30, 7621–7623.
7. Zhao, Y.; Lei, H. *Macromolecules* 1992, 25, 4043–4045.
8. Chen, S.; Du, C.; Jin, Y.; Qian, R.; Zhou, Q. *Mol Cryst Liq Cryst* 1990, 188, 197–205.
9. Kang, E. T.; Neoh, K. G.; Masuda, T.; Higashimura, T.; Yamamoto, M. *Polymer* 1989, 30, 1328–1331.
10. Masuda, K.; Akagi, K.; Shirakawa, H.; Nishizawa, T. *J Mol Struct* 1998, 441, 173–181.
11. Tang, B. Z.; Kong, X.; Wan, X.; Peng, H.; Lam, W. Y. *Macromolecules* 1998, 31, 2419–2432.
12. Moigne, J. L.; Hiberer, A. *Makromol Chem* 1991, 192, 515–530.
13. Hasegawa, H.; Kijima, M.; Shirakawa, H. *Synth Met* 1997, 84, 177–178.
14. Kijima, M.; Abe, S.; Shirakawa, H. *Synth Met* 1999, 101, 61.
15. Toyoshima, R.; Narita, M.; Akagi, K.; Shirakawa, H. *Synth Met* 1995, 69, 289–290.

16. Dai, X. M.; Goto, H.; Akagi, K.; Shirakawa, H. *Synth Met* 1999, 102, 1291.
17. Dai, X. M.; Narihiro, H.; Goto, H.; Akagi, K.; Yokoyama, H. *Synth Met* 2001, 119, 397–398.
18. Kong, X.; Tang, B. Z. *Chem Mater* 1998, 10, 3352–3363.
19. Geng, J.; Zhao, X.; Zhou, E.; Li, G.; Lam, J. W. Y.; Tang, B. Z. *Polymer* 2003, 44, 8095–8102.
20. Akagi, K.; Goto, H.; Kadokura, Y.; Shirakawa, H.; Oh, S. Y.; Araya, K. *Synth Met* 1995, 69, 13–16.
21. Goto, H.; Akagi, K. *Synth Met* 1999, 102, 1292.
22. Osaka, I.; Shibata, S.; Toyoshima, R.; Akagi, K.; Shirakawa, H. *Synth Met* 1999, 102, 1437–1438.
23. Osaka, I.; Goto, H.; Itoh, K.; Akagi, K. *Synth Met* 2001, 119, 541–542.
24. Kong, X.; Lam, W. Y.; Tang, B. Z. *Polym Mater Sci Eng* 1999, 80, 151–152.
25. Geng, J.; Geng, F.; Wang, J.; Zhu, B.; Li, G.; Zhou, E.; Lam, J. W. Y.; Tang, B. Z. *Liq Cryst*, in press.
26. Geng, J.; Zhao, X.; Zhou, E.; Li, G.; Lam, J. W. Y.; Tang, B. Z. *Mol Cryst Liq Cryst* 2003, 399, 17–28.
27. Finkelmann, H.; Ringsdorf, H.; Wendorff, J. H. *Makromol Chem* 1978, 179, 273–276.
28. Finkelmann, H.; Ringsdorf, H.; Siol, W.; Wendorff, J. H. *Makromol Chem* 1978, 179, 829–832.